Development 106, 427–439 (1989)
Printed in Great Britain © The Company of Biologists Limited 1989

Roles of neuroepithelial cell rearrangement and division in shaping of the avian neural plate

GARY C. SCHOENWOLF and IGNACIO S. ALVAREZ*

Department of Anatomy, University of Utah, School of Medicine, Salt Lake City, Utah, 84132, USA

* Permanent address: Departamento de Ciencias Morfológicas y Biología Celular y Animal, Facultad de Ciencias, Universidad de Extremadura, 06071 Badajoz, Spain

Summary

Shaping of the neural plate, one of the most striking events of neurulation, involves rapid craniocaudal extension. In this study, we evaluated the roles of two processes in neural plate extension: neuroepithelial cell rearrangement and cell division. Quail epiblast plugs of constant size were grafted either just rostral to Hensen's node or paranodally and the resulting chimeras were examined at selected times postgrafting. By comparing the size of the original plug, the number of cells it contained and the distribution of cells within it to those same features of the grafts in chimeras, we were able to ascertain that, during transformation of the flat neural plate into the closed neural tube (a period requiring 24 h), the graft undergoes a maximum of 3 rounds of craniocaudal extension (each round of craniocaudal extension was defined as a doubling of graft length, so 3 rounds equaled an 8-fold increase in length). Such extension is accompanied by 2 rounds of cell rearrangement and 2–3 rounds of cell division (cell rearrangement occurred mediolaterally, so each round was defined as a halving of the number of cells in the width of the graft and a doubling of the number of cells in its length; each round of cell division was defined as a doubling of graft cell number). Modeling studies demonstrate that these amounts of cell rearrangement and division are sufficient to approximate the shaping of the neural plate that normally ensues during neurulation, provided that some of the cell division occurs within the longitudinal plane of the neural plate and some within its transverse plane: longitudinal cell division results in craniocaudal extension of the neural plate, whereas transverse cell division results in lateral expansion of the neural plate such as that occurring at its cranial end; cell rearrangement results in craniocaudal extension of the neural plate as well as in its narrowing. In conclusion, our results provide evidence that shaping of the neural plate involves mediolateral cell rearrangement and cell division, with the latter occurring within both the longitudinal and transverse planes of the neural plate.

Key words: avian embryos, cell division, cell rearrangement, chimeras, neural plate, neurulation.

Introduction

Shortly after formation of the neural plate, a series of morphogenetic events occurs that culminates in formation of the neural tube (reviewed by Schroeder, 1970; Burnside, 1973; Karfunkel, 1974; Schoenwolf, 1982; Gordon, 1985; Martins-Green, 1988). During the first of these, shaping of the neural plate, the neural plate, on the average, thickens dorsoventrally, narrows mediolaterally and extends craniocaudally. Bending of the neural plate begins during shaping. In this process, the neural folds form at the lateral margins of the neural plate and elevate, delimiting the neural groove. Continued elevation of the neural folds, as well as their convergence, results in their apposition in the dorsal midline where they fuse, thereby closing the neural groove and establishing the neural tube.

The cellular and molecular mechanisms underlying neural tube formation are poorly understood. The present study was designed to examine the cellular events involved in neural plate *shaping*. This process has been studied over the last 20 years in amphibians (Burnside & Jacobson, 1968; Schroeder, 1971; Jacobson & Gordon, 1976; Suzuki & Harada, 1988), birds (Schoenwolf, 1985, 1988; Schoenwolf & Powers, 1987; Schoenwolf & Sheard, 1989; Schoenwolf *et al.* 1988, 1989*a*,*b*) and mammals (Morriss-Kay, 1981; Morriss-Kay & Tuckett, 1987; Tuckett & Morriss-Kay, 1985). Although experimental data are available on the mechanisms of neural plate *thickening* and *narrowing* (see review by Karfunkel, 1974; Schoenwolf & Powers, 1987), our understanding of neural plate *extension* is based mainly on speculation. Two mechanisms are

usually considered to be at the forefront: neuroepithelial cell rearrangement and cell division.

Cell rearrangement plays a major role in convergent extension during *Xenopus* gastrulation (reviewed by Keller *et al.* 1985). Similarly, neuroepithelial cell rearrangement likely occurs during neural plate shaping (Jacobson & Gordon, 1976; Morriss-Kay & Tuckett, 1987; Schoenwolf & Sheard, 1989; Schoenwolf *et al.* 1989*a*), but its magnitude, direction, regional differences and exact role remain largely unknown. The present study, based on mapping the displacement of grafted cells, documents mediolateral cell rearrangement throughout the avian neural plate and estimates its magnitude.

Cell division plays an important role in the morphogenesis of higher vertebrates in which extensive growth occurs during early embryogenesis. Neural plate cells undergo rapid proliferation during neural plate shaping and bending, becoming postmitotic only after the neural groove has closed (Langman *et al.* 1966; Tuckett & Morriss-Kay, 1985; Smith & Schoenwolf, 1987, 1988). In the present study, the amount of cell division in the neural plate is estimated by determining the numbers of cells derived over time from grafts of known cell number. This information was combined with that obtained on cell rearrangement to model the relative contributions of cell rearrangement and cell division in regional shaping of the avian neural plate.

Materials and methods

Plugs of quail epiblast were transplanted homotopically and isochronically to chick blastoderms developing in whole embryo culture. After further development, the resulting chimeras were examined histologically and sections were analyzed quantitatively.

Experimental procedures

Quail/chick chimeras were constructed using the methods described previously (Schoenwolf *et al.* 1989*a*). Chick blastoderms were used as hosts and quail blastoderms as donors. Briefly, chick blastoderms at Hamburger and Hamilton's (1951) stage 3 (specifically, stages 3c and 3d as described by Schoenwolf, 1988) were cultured dorsal side down in modified New (1955) culture. The endoderm covering the cranial part of the blastoderm was detached from the area opaca and reflected caudally. A circular hole was punched with the polished tip of a pipette (190 μm i.d.) through the exposed epiblast at the prospective graft site (Fig. 1). The same pipette was used to remove a comparable plug from a quail epiblast at the same stage. The quail plug was then transferred to the host blastoderm and inserted into the graft site (with the appropriate dorsal–ventral orientation); the previously reflected host endoderm was replaced, covering the graft (Fig. 2). Blastoderms were reincubated for 4–24 h (at 2 h periods) and then fixed, processed for histology, serially sectioned transversely at 5 μm and stained with the Feulgen–Rossenbeck procedure as described by Lillie (1965).

Schoenwolf *et al.* (1989*a*) showed previously that midline grafts rostral to Hensen's node (site 'a') formed much of the forebrain as well as median wedge cells (M cells) of the midbrain through spinal cord, whereas lateral grafts to the flanks of Hensen's node (site 'b') contributed to the lateral walls (L cells) of the entire neuraxis. In the present study, we grafted plugs of *constant* diameter to these same sites to examine neuroepithelial cell rearrangement and cell division during shaping of the neural plate. These sites were chosen to allow us to compare the behavior of M and L cells throughout all subdivisions of the neuraxis.

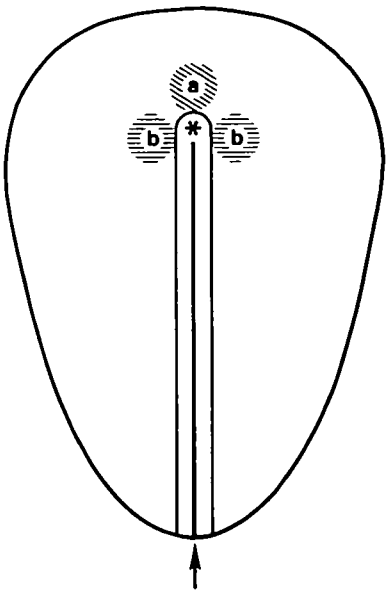

Fig. 1. Schematic representation of the sites where quail epiblast plugs were grafted to chick epiblasts. Grafts at site 'a' were placed with their caudal boundary as much as 100 μm *cranial* to the cranial border of Hensen's node (asterisk). Similarly, grafts at site 'b' were placed with their medial boundary as much as 100 μm *lateral* to the lateral borders of Hensen's node and with their cranial boundary as much as 100 μm cranial to the cranial border of Hensen's node. An approximately equal number of grafts at site 'b' were done on the right and left sides of Hensen's node. Arrow indicates the caudal end of the primitive streak. The illustration was modified from Schoenwolf *et al.* 1989*a*: fig. 1).

Isolated plugs of quail epiblast, as well as chimeras, were analyzed histologically. To do this, plugs were fixed immediately after their removal from quail blastoderms and transferred to melted agar (1·5% Bacto-Agar, Difco Labs, Detroit, in distilled water). The agar was solidified by cooling, cut into small rectangular blocks (each of which contained a plug) and fixed. Blocks were then processed for histology, serially sectioned and stained in a manner similar to that described for the chimeras.

Quantitative procedures

In sections, the presence of densely stained nucleolar-associ-

Table 1. *Numbers of quail epiblast plugs and quail/chick chimeras selected for quantitative analysis*

	Time postgrafting				
	Plugs	Chimeras			
	0 h	8 h	12 h	18 h	24 h
Site 'a'	6	2	4	4	5
Site 'b'	10	0	3	7	5

Table 2. *Quantitative analyses of quail epiblast* plugs

Sites	Mean diameters of nucleolar markers μm	Mean numbers of cells in plugs	Mean diameters of plugs μm	Mean heights of plugs μm	Mean lengths of plugs μm	Calculated volumes of plugs† μm^3	Mean numbers of cells occupying diameters of plugs
'a'	2·1 ± 0·1*	285 ± 19	161 ± 10	35 ± 0·8	161 ± 11	712 542	20 ± 2
'b'	2·3 ± 0·1	302 ± 15	168 ± 7	32 ± 0·6	147 ± 6	709 348	21 ± 1

* Standard error of the mean.

† Plugs were considered to be cylinders and volumes were calculated according to the following formula: $\pi r^2 h$; r (radius) was calculated from the diameter, not from the length, because the latter could be underestimated due to compression during sectioning and the loss of sections or the failure to count tangential sections through the graft; h, height.

ated heterochromatin was used to identify quail cells (LeDouarin, 1982). Ninety-nine chimeras were made; 30 of these were selected for quantitative analysis (Table 1). Selection was based on when the culture was terminated (i.e. we quantitatively analyzed only those grafts obtained from chimeras at 8, 12, 18, and 24 h postgrafting) and whether the graft incorporated completely, development of the blastoderm occurred normally and the histology was of good quality. Also, to keep the data set manageable, some chimeras that met these criteria were not studied quantitatively. 16 plugs were selected from the 18 collected, based solely on the quality of the histology (Table 1).

A variety of parameters was assessed on serial sections. We began with quail epiblast *plugs* (Table 2). First, we determined the mean numbers of cells in plugs obtained from sites 'a' and 'b.' To do this, we counted nuclei containing nucleolar markers (when two markers were present in a single nucleus only one was scored) in *every* serial section through each plug, and the number of nuclei with markers in each plug was calculated. These values were then corrected according to the method of Abercrombie (1946) using correction factors obtained from measurements (with an eyepiece micrometer) of the transverse diameters of 200 nucleolar markers (50 nuclei containing markers were chosen in each of 4 randomly selected plugs, 2 obtained from site 'a' and 2 from site 'b'). Second, we determined the mean plug diameters (from measurements of the greatest 'width' of each plug), heights (from measurements of the greatest apicobasal extent of each plug in every *fifth* serial section) and lengths (from counts of the number of 5 μm sections through each plug) and used the diameters and heights to calculate plug volumes. Plug volumes were compared to the total volume of the neural plate (data from Schoenwolf, 1985) to estimate the percentage of the volume of the neural plate grafted. Finally, we determined the mean numbers of cells occupying the diameters of plugs, by counting the number of nuclei containing nucleolar markers in the greatest width of each plug.

Next, *chimeras* were analyzed in ways similar to those used for plugs (Tables 3, 4). First, we determined the mean numbers of cells in grafts at sites 'a' and 'b' at selected times postgrafting (i.e. at 8, 12, 18 and 24 h), using counts of nuclei containing nucleolar markers and the previously calculated correction factors. Nuclei with markers were counted in every other section when the graft extended less than 50 sections, in every third section when it extended 50–100 sections, in every fourth section when it extended 100–200 sections and in every fifth section when it extended for more than 200 sections. The mean numbers of cells in grafts were then compared to the previously determined mean numbers of cells in plugs to estimate the numbers of rounds of cell division that had occurred by each time postgrafting (Table 3). One round of cell division was defined as a doubling of the graft cell number. Second, we determined the mean lengths of grafts from counts of the number of 5 μm sections through each graft. We then compared these values to those determined previously for plugs to estimate the numbers of rounds of craniocaudal extension (Table 3). One round of craniocaudal extension was defined as a doubling of the graft length. We noted that the lengths of grafts varied considerably within each time period postgrafting, so that the length of the graft and its age were not always correlated, and the length of the graft also was often not correlated with the number of cells contained in it (see Results). We regrouped the data according to the length of the graft rather than to the time postgrafting (Table 4). Length categories were chosen by comparing the lengths of the grafts to the lengths of the plugs, so that categories delineated 0–3 rounds of craniocaudal extension. Third, we determined the mean numbers of cells in

Table 3. *Quantitative analyses of quail epiblast grafts obtained from* chimeras *grouped according to the time postgrafting*

Sites	Mean numbers of cells in grafts	Rounds of cell division†	Mean lengths of grafts μm	Rounds of craniocaudal extension‡
'a'				
8 h	371 ± 60*	0	220 ± 70	0
12 h	525 ± 87	1	256 ± 46	1
18 h	964 ± 54	2	641 ± 147	2
24 h	1325 ± 491	2	314 ± 69	1
'b'				
12 h	724 ± 98	1	581 ± 181	2
18 h	1094 ± 413	2	918 ± 165	3
24 h	1288 ± 576	2	1101 ± 262	3

* Standard error of the mean.

† The numbers of rounds of cell division are each rounded to the nearest whole number. The values 570, 1140 and 2280 represent, respectively, 1, 2 and 3 rounds of cell division for grafts at site 'a' (plugs obtained from site 'a' have a mean of 285 cells, so 1 round of cell division would result in a graft with 570 cells; Table 2); 604, 1208 and 2416 represent, respectively, 1, 2 and 3 rounds of cell division for grafts at site 'b' (plugs obtained from site 'b' have a mean of 302 cells, so 1 round of cell division would result in a graft with 604 cells; Table 2).

‡ The number of rounds of craniocaudal extension are each rounded to the nearest whole number. The values 322 and 644 represent, respectively, 1 and 2 rounds of craniocaudal extension for grafts at site 'a' (plugs obtained from site 'a' have a mean length of 161 μm, so 1 round of extension would result in a graft with a length of 322 μm; Table 2); 294, 588 and 1176 represent, respectively, 1, 2 and 3 rounds of craniocaudal extension for grafts at site 'b' (plugs obtained from site 'b' have a mean length of 147 μm, so 1 round of extension would result in a graft with a length of 294 μm; Table 2).

the widths of the midcraniocaudal extents of the grafts. To do this, the numbers of cells in the widths of the grafts in transverse sections were determined. Values were grouped according to their location in one of five equally spaced craniocaudal positions along the length of the graft. The value obtained from the midcraniocaudal extent of each graft was divided by the number of sections analyzed in this region and it was then compared to the numbers of cells in the diameters of the plugs to estimate the numbers of rounds of mediolateral cell rearrangement (Table 4). A graft whose cells undergo 1 round of mediolateral rearrangement would be expected to halve its width and double its length in a manner similar to that depicted elsewhere (Keller & Hardin, 1987: Fig. 1). Stated in another way, 1 round of cell rearrangement would result, by definition, in a halving of the number of cells in its transverse plane and a doubling of the number of cells in its longitudinal plane. Finally, the mediolateral positions of grafts in transverse sections were determined by measuring the distances of their edges from the midline along the midapicobasal extent of the neural plate in every *fifth* (graft less than 300 μm in length) or *tenth* (graft greater than 300 μm in length) serial section. An Apple II+ computer was used to reconstruct the grafts, and an Apple MacIntosh SE was used for modeling.

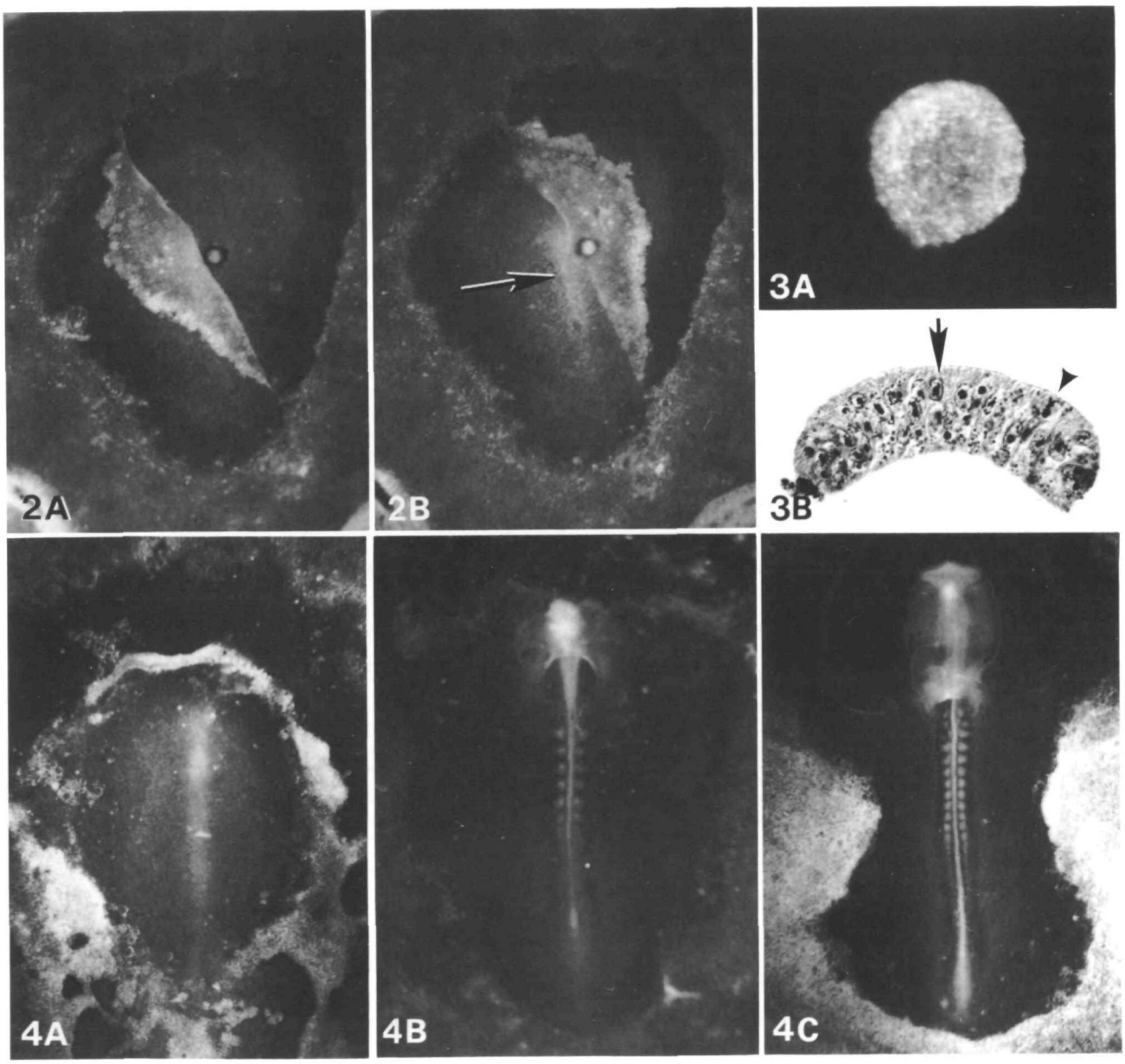

Fig. 2. Ventral views of a chick blastoderm in whole-embryo culture just after receiving a quail epiblast graft at site 'b.' The endoderm is still reflected in Fig. 2A but has been replaced in Fig. 2B. Arrow indicates the primitive streak. ×30 approx.
Fig. 3. Quail epiblast plug viewed from its basal (ventral) side at the time of isolation (Fig. 3A) or in transverse section after fixation and processing for histological study (Fig. 3B). Arrow indicates the *apical* side of plug; arrowhead indicates a mitotic figure. A, ×130 approx.; B, ×290.
Fig. 4. Ventral views of chick blastoderms in whole-embryo culture at 4 h (Fig. 4A), 12 h (Fig. 4B) and 24 h (Fig. 4C) after receiving a quail epiblast graft. ×30 approx.

Table 4. *Quantitative analyses of quail epiblast grafts obtained from* chimeras *grouped according to the length of the graft*

Sites	Numbers of chimeras	Lengths of grafts μm†	Rounds of craniocaudal extension	Mean numbers of cells in widths of the midcraniocaudal extents of grafts	Rounds of cell rearrangement‡	Mean numbers of cells in grafts	Rounds of cell division§
'a'	5	<264	0	29 ± 3*	0	591 ± 74	1
	7	264–483	1	17 ± 2	0	910 ± 178	2
	3	483–966	2	5 ± 1	2	998 ± 132	2
'b'	4	294–441	1	21 ± 3	0	751 ± 107	1
	2	441–882	2	12 ± 2	1	1022 ± 97	2
	9	882–1764	3	7 ± 1	2	1404 ± 169	2

*Standard error of the mean.

†Length categories delineate 0–3 rounds of craniocaudal extension. For example, for grafts at site 'a', a graft exhibiting no extension would have a length of 161 μm (i.e. the mean length of the plug; Table 2), and one exhibiting 1 round of extension would have a length of 322 μm. The value 264 is midway between 161 and 322; we considered grafts with lengths greater than 264 to have undergone 1 round of elongation and those with less than this to have undergone 0 rounds.

‡The numbers of rounds of cell rearrangement are each rounded to the nearest whole number; 10 and 5 represent, respectively, 1 and 2 rounds of cell rearrangement for grafts at both sites 'a' and 'b' (plugs obtained from site 'a' have a mean of 20 cells in their diameters and those from site 'b' have a mean of 21, so 1 round of cell rearrangement would result in a graft with 10 cells in its midcraniocaudal width; Table 2).

§The numbers of rounds of cell division are each rounded to the nearest whole number; 570, 1140 and 2280 represent, respectively, 1, 2 and 3 rounds of cell division for grafts at site 'a' (plugs obtained from site 'a' have a mean of 285 cells, so 1 round of cell division would result in a graft with 570 cells; Table 2); 604, 1208 and 2416 represent, respectively, 1, 2 and 3 rounds of cell division for grafts at site 'b' (plugs obtained from site 'b' have a mean of 302 cells, so 1 round of cell division would result in a graft with 604 cells; Table 2).

Results

Quantitative analyses of quail epiblast plugs

Epiblast plugs were isolated from quail blastoderms, fixed and processed for histology (Fig. 3). Sections were used to assess several parameters (Table 2). For plugs obtained from sites 'a' and 'b,' the mean diameters of the nucleolar markers were similar (2·1 and 2·3 μm, respectively). Likewise, the mean numbers of cells in plugs (285 and 302, respectively), the mean diameters of plugs (161 and 168 μm, respectively), the mean heights of plugs (35 and 32 μm, respectively), the mean lengths of plugs (161 and 147 μm, respectively) and the mean numbers of cells across the diameters of plugs (20 and 21, respectively) were similar. The calculated volumes of the plugs, when compared to data obtained previously (Schoenwolf, 1985), indicated that each plug had a volume of about 5% of that of the entire neural plate.

General developmental features of chimeras

Examination of chimeras at periods ranging from 4–24 h postgrafting revealed that grafting did not adversely affect the overall development of host embryos (Fig. 4). Although there was considerable variation, embryos usually reached stages 4–5 by 4 h postgrafting, 7–9 by 12 h postgrafting and 10–12 by 24 h postgrafting. Healing of the graft into the host's neuroepithelium occurred rapidly. By 4–6 h, about half the grafts had healed in place (Fig. 5) and by 8 h, virtually all the grafts had healed.

The fates of cells grafted to sites 'a' and 'b' were identical to those reported previously (Schoenwolf *et al.*

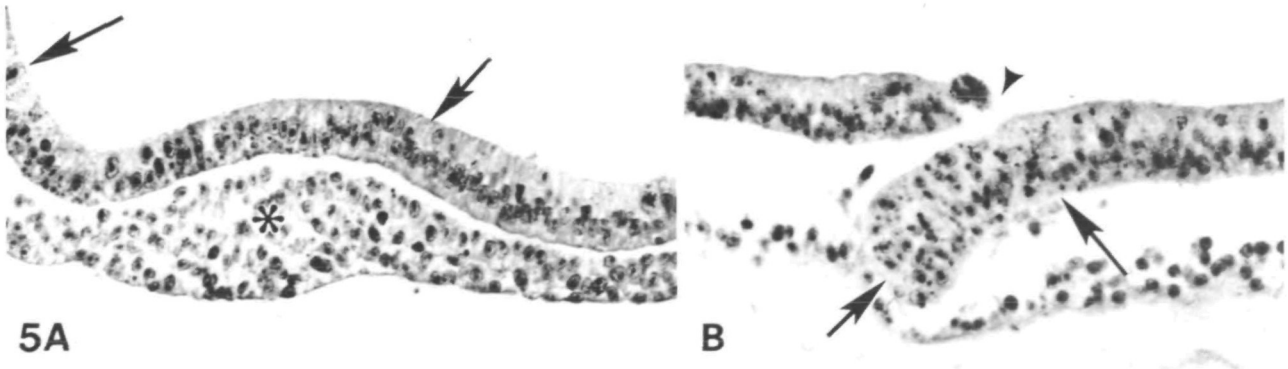

Fig. 5. Transverse sections through chimeras fixed 4 h after receiving quail epiblast grafts at site 'a' (Fig. 5A) and 'b' (Fig. 5B). In Fig. 5A, the graft has completely incorporated into the neuroepithelium and overlies the head process (asterisk), but in Fig. 5B, incorporation is still incomplete (arrowhead). Arrows indicate the mediolateral extents of the quail grafts. ×150.

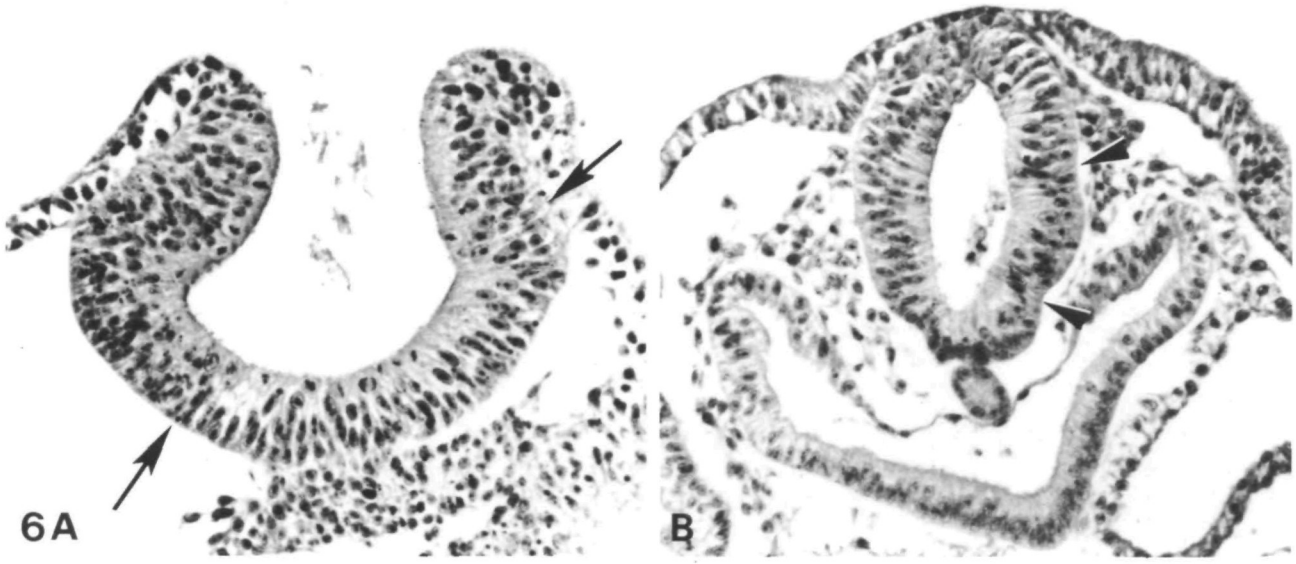

Fig. 6. Transverse sections through chimeras fixed 24 h after receiving a quail epiblast graft at site 'a' (Fig. 6A) or site 'b' (Fig. 6B). Arrows indicate the mediolateral extent of the quail graft in the floor and lateral wall of the forebrain; arrowheads indicate the mediolateral extent of the quail graft in the lateral wall of the hindbrain. ×200.

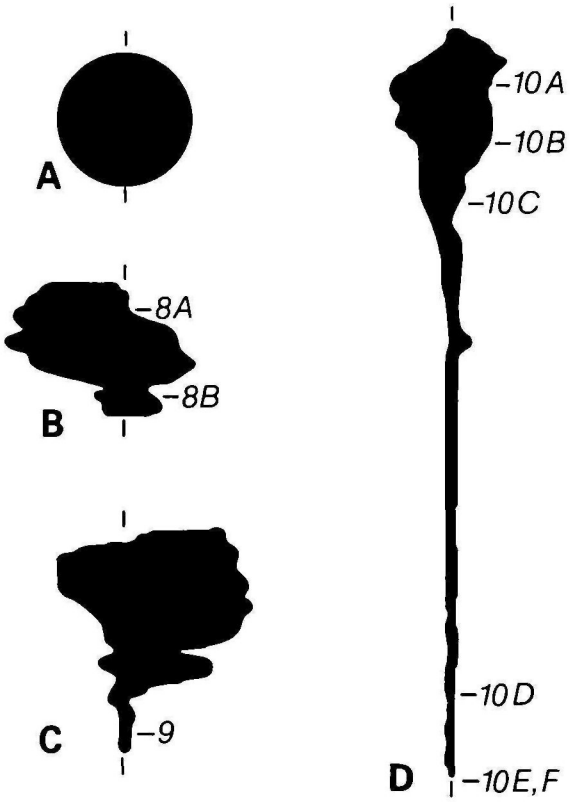

Fig. 7. Reconstructions of grafts at site 'a.' Vertical lines indicate the midline. Fig. 7A shows the original graft to indicate the scale (diameter = 161 μm; Table 2). The graft reconstructed in Fig. 7B was fixed 24 h postgrafting; it contained 657 cells and underwent 0 rounds of craniocaudal extension (length = 160 μm). The graft reconstructed in Fig. 7C was fixed 18 h postgrafting; it contained 851 cells and underwent 1 round of craniocaudal extension (length = 285 μm). The graft reconstructed in Fig. 7D was fixed 18 h postgrafting; it contained 904 cells and underwent 2 rounds of craniocaudal extension (length = 920 μm). Levels of sections shown in Figs 8–10 are indicated by labeled horizontal lines.

1989*a*); namely, grafts at site 'a' contributed to the floor and much of the lateral walls of the forebrain, as well as to M cells of the midbrain through spinal cord (Fig. 6A), whereas grafts at site 'b' contributed to L cells of the lateral walls of the forebrain through spinal cord (Fig. 6B). Grafts at site 'b' sometimes contributed a few M cells to the caudal spinal cord. Because the *exact* placement of grafts varied within each site (Fig. 1), it was likely that such grafts slightly overlapped the prospective M cell territory usually mapped by grafts at site 'a'.

Quantitative analysis of grafts

As in the previous study (Schoenwolf *et al.* 1989*a*), the exact distribution of grafted cells varied considerably (Figs 7–14). Reconstructions of the grafts demonstrated that their shapes also varied (Figs 7, 11).

Grafts at site 'a' retained their midline positions. As grafts extended caudally, their shapes changed from circular to club-like, so that the most extended grafts showed marked tapering craniocaudally (Fig. 7D). Comparison of the shapes of the extended grafts with that of the original plug showed that craniocaudal extension was accompanied by mediolateral narrowing (cf. Fig. 7A, D).

Sections through grafts at site 'a' revealed a strong correlation between the precise level where the graft was placed and the final craniocaudal and mediolateral distributions of its cells. Grafts contributing principally to the forebrain expanded laterally with formation of

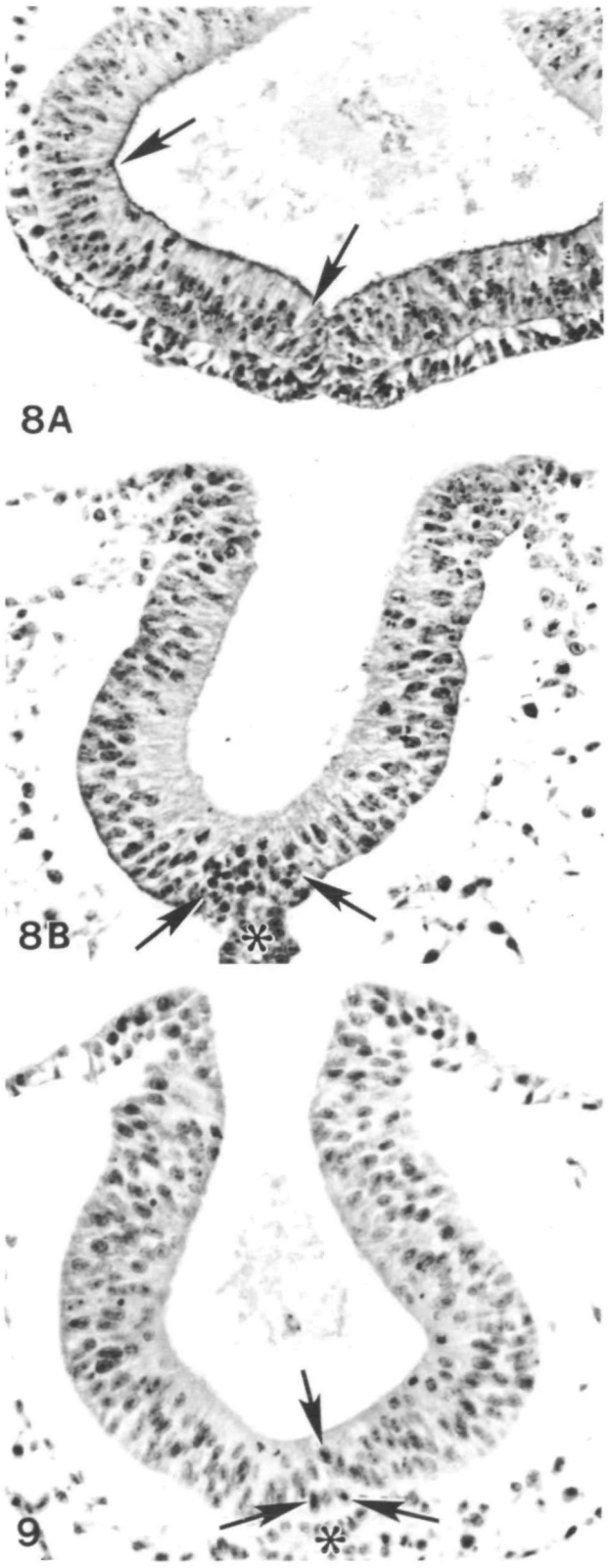

Fig. 8. Transverse sections through the graft reconstructed in Fig. 7B; see Fig. 7B for section orientation. Fig. 8A, forebrain level; Fig. 8B, midbrain level. Arrows indicate the mediolateral extents of the quail grafts; asterisk indicates the notochord. ×200.

Fig. 9. Transverse section through the graft reconstructed in Fig. 7C; see Fig. 7C for section orientation. Arrows indicate quail M cells in the floor of the midbrain; asterisk indicates the cranial end of the notochord. ×200.

the optic vesicles and contained many cells in their mediolateral extents (Figs 7B, 7C, 8A, 10A). In contrast, grafts contributing to the midbrain (this level of the neuraxis is indicated by the presence of the cranial tip of the notochord and the fading out of the optic vesicles) and more caudal levels of the neuraxis (i.e. hindbrain, as indicated by narrowing of the brain and the appearance of the otic vesicles; spinal cord, that level of the neuraxis caudal to the fifth pair of somites) were mediolaterally narrowed, craniocaudally extended and composed of few cells (Figs 7B, C, 8B, 9, 10B–F). Near the caudal ends of most grafts, gaps (i.e. regions containing only chick cells) appeared in their craniocaudal extents, so that some sections contained quail cells and others only chick (cf. Fig. 10D–F). A more craniocaudally extended graft was more likely to show gaps than was a less-extended one. Regions of the grafts showing gaps routinely exceeded 100 μm and reached as much as 300 μm, and gaps often spanned several contiguous sections.

Grafts at site 'b' did not maintain their original mediolateral positions. Rather, these grafts moved medially (Fig. 11C,D) in all but a few cases. In the few exceptions, the cranial part of each graft moved laterally, whereas its caudal part moved medially (Fig. 11B). Like grafts at site 'a,' grafts at site 'b' showed marked tapering craniocaudally, and craniocaudal extension was accompanied by mediolateral narrowing (Fig. 11B–D).

Sections through grafts at site 'b' also revealed a strong correlation between the precise level where the graft was placed and the final craniocaudal and mediolateral distributions of its cells. In the few cases where the cranial parts of the grafts moved laterally, their cells contributed to the lateral walls of the forebrain, including the optic vesicles (Figs 11B, 12A), or to the lateral walls of the midbrain. The more caudal parts, which moved medially, contributed to the lateral walls of the midbrain (Figs 11B, 12B) or hindbrain. The remaining grafts, all of which moved medially in their entirety, began at the level of the mid- or hindbrain (Figs 11C,D, 13, 14A) and typically extended caudally throughout the spinal cord (Figs 11D, 14B). As was the case for grafts at site 'a,' gaps were present in the craniocaudal extents of most grafts at site 'b' near their caudal ends.

Serial sections of grafts obtained from chimeras were analyzed quantitatively in the same manner as that used for quail epiblast plugs. Initially, data were grouped according to the time postgrafting (Table 3). Such a grouping revealed that cell number had doubled by 12 h postgrafting (i.e. 1 round of cell division) in grafts at both sites 'a' and 'b,' and that a second doubling had occurred by 18 h postgrafting. A third doubling did not occur during the 24 h postgrafting period. The lengths of the grafts, like the numbers of cells in them, tended to increase over time, but graft length, graft age and cell

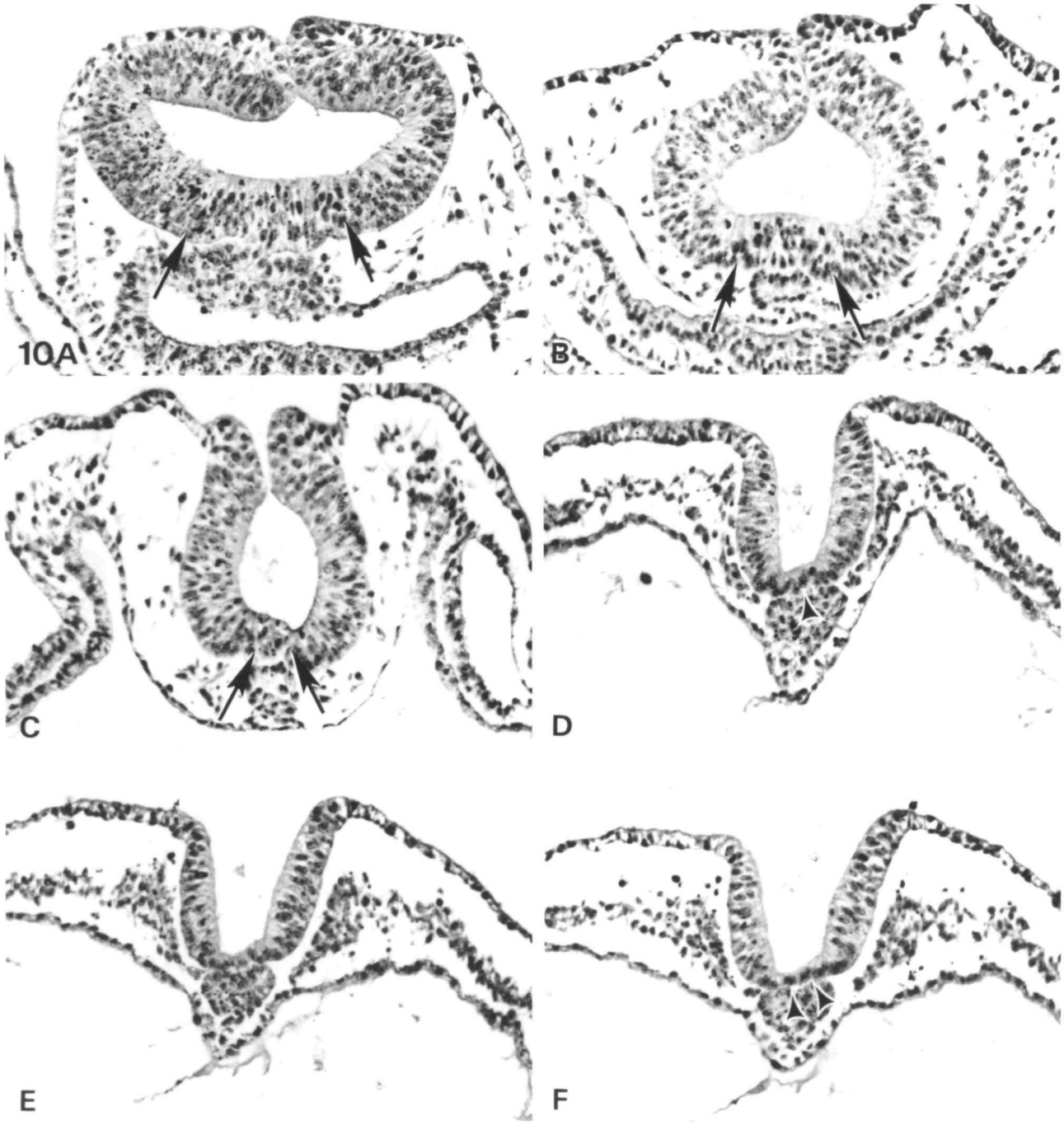

Fig. 10. Transverse sections through the graft reconstructed in Fig. 7D; see Fig. 7D for section orientation. Fig. 10A, caudal forebrain; Fig. 10B, midbrain; Fig. 10C, hindbrain; Fig. 10D–F, caudal spinal cord. Gaps occur in the craniocaudal extent of the graft near its caudal end, so that quail M cells (arrowheads) are present at some levels (Fig. 10D,F) but not at intervening levels (Fig. 10E). Arrows indicate the mediolateral extents of the quail graft. ×200.

number were not completely correlated. This was especially evident for grafts at site 'a' in which at 12 h postgrafting, the grafts were composed of a mean of 525 cells and had attained a mean length of 256 μm, whereas at 24 h, cell number had almost tripled but graft length had only increased slightly (Table 3).

Data were regrouped according to the length of the graft (Table 4). Grafts at sites 'a' and 'b' underwent 0–3 rounds of craniocaudal extension. Grafts at site 'a' extending 0 rounds contributed almost exclusively to the forebrain, those extending 2 rounds contributed only a few (or no) cells to the forebrain and those extending 1 round contributed to the forebrain to an intermediate extent. Grafts at site 'a' that contributed almost exclusively to the forebrain (and underwent 0 rounds of craniocaudal extension) expanded laterally and increased the numbers of cells contained within their widths (Table 4, 29 cells in the widths of the

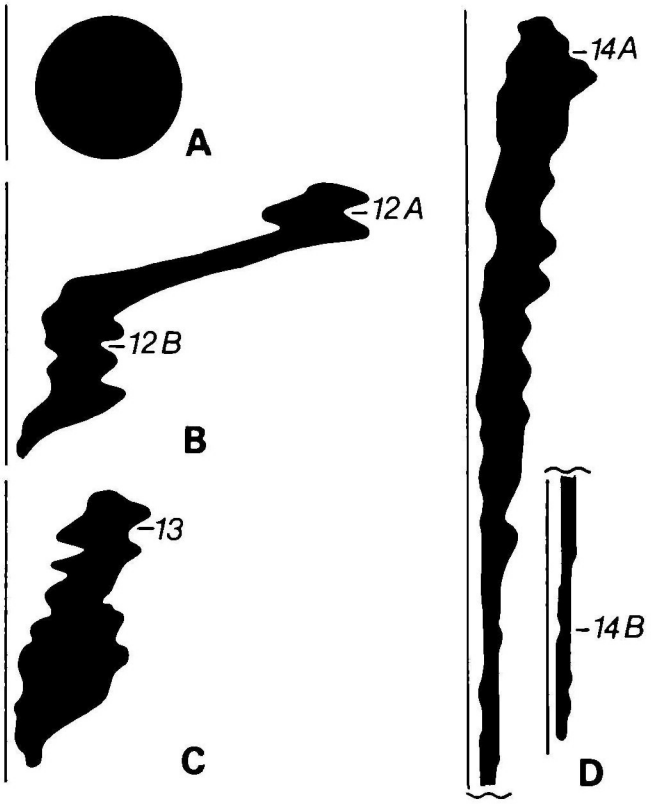

Fig. 11. Reconstructions of grafts at site 'b.' Vertical lines indicate the midline. Fig. 11A shows the original graft to indicate the scale (diameter = 168 μm; Table 2). The graft reconstructed in Fig. 11B was fixed 18 h postgrafting; it contained 790 cells and underwent 1 round of craniocaudal extension (length = 345 μm). The graft reconstructed in Fig. 11C was fixed 24 h postgrafting; it contained 1103 cells and underwent 1 round of craniocaudal extension (length = 375 μm). The graft reconstructed in Fig. 11D was fixed 24 h postgrafting; it contained 1554 cells and underwent 3 rounds of craniocaudal extension (length = 1250 μm). Levels of sections shown in Figs 12–14 are indicated by labeled horizontal lines.

midcraniocaudal extents of the grafts, 0 rounds of cell rearrangement), whereas those that underwent substantial craniocaudal extension (and contributed to the forebrain to little or no extent) narrowed mediolaterally and had cells that underwent rearrangement (Table 4, 2 rounds of cell rearrangement). In grafts undergoing 1 and 2 rounds of craniocaudal extension, 2 rounds of cell division occurred (Table 4).

Grafts at site 'b' underwent 1–3 rounds of craniocaudal extension (Table 4). In the few cases in which the cranial parts of grafts contributed to the forebrain, only 1 round of craniocaudal extension and 0 rounds of cell rearrangement occurred (Table 4). In the remaining cases, the grafts underwent considerable craniocaudal extension (Table 4, 2 or 3 rounds of craniocaudal extension). Such extension was accompanied by mediolateral narrowing of the graft and rearrangement of its cells (Table 4, 1 or 2 rounds of cell rearrangement). In grafts undergoing 2 and 3 rounds of craniocaudal extension, 2 rounds of cell division occurred (Table 4).

Discussion

Shaping of the neural plate is a prominent event of neurulation during which the initially lunate neural plate transforms into a spatulate rudiment. Shaping involves three major changes in the neural plate: on the average, the neural plate *thickens* in the dorsoventral plane, *narrows* in the mediolateral plane and *extends* in the craniocaudal plane. A principal question being addressed in our laboratory is: what are the cellular and molecular processes underlying these morphological events? Below, we will discuss three major questions whose answers provide some insight. Then, we will present a model that portrays one possible way in which the identified cellular protagonists may band together to shape the neural plate.

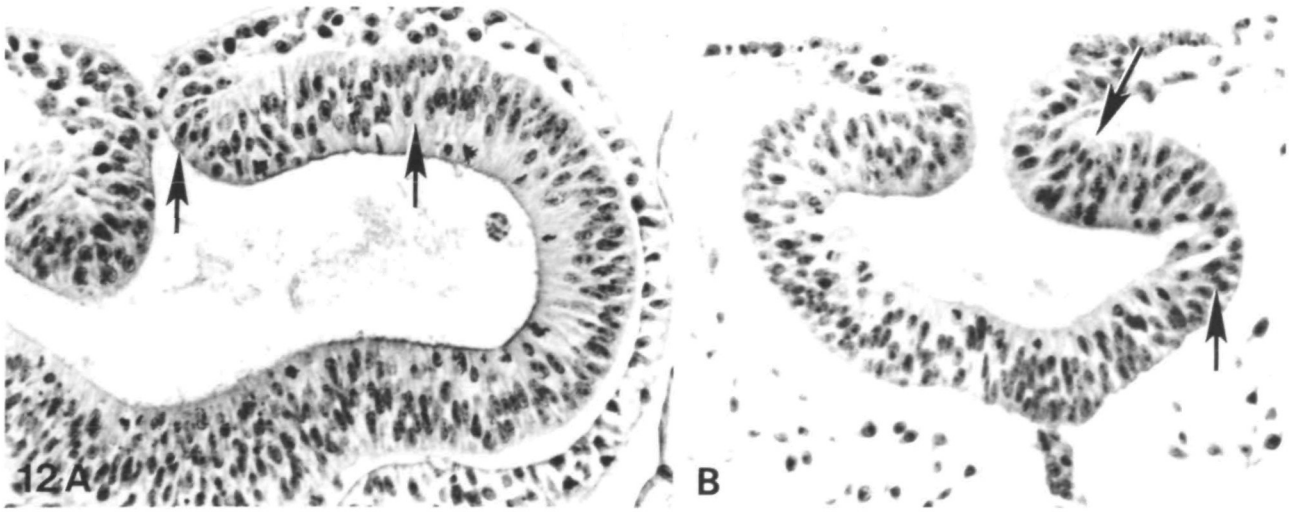

Fig. 12. Transverse sections through the graft reconstructed in Fig. 11B; see Fig. 11B for section orientation. Fig. 12A, forebrain level; Fig. 12B. midbrain level. Arrows indicate the mediolateral extents of the quail grafts. ×200.

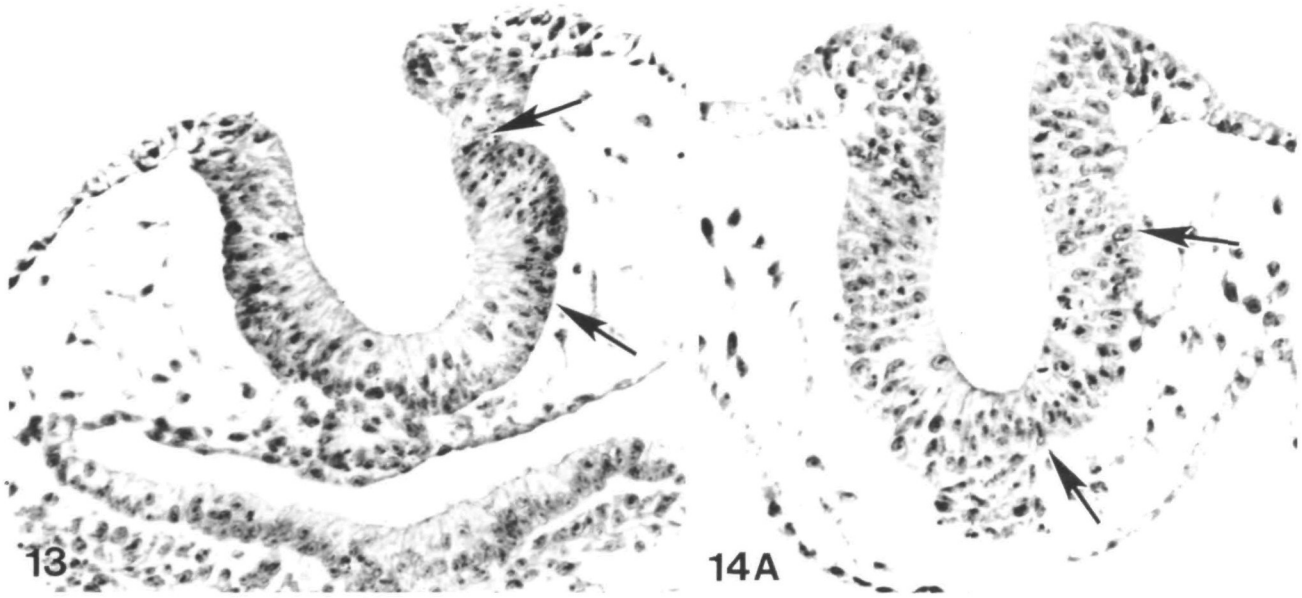

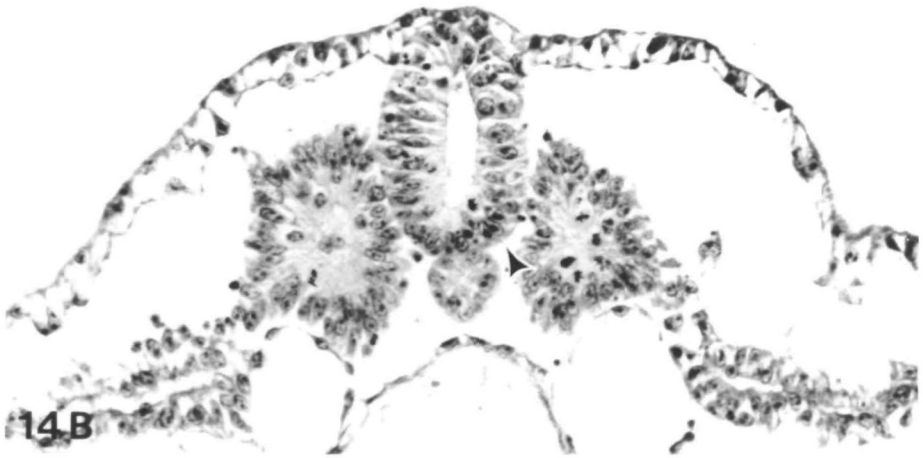

Fig. 13. Transverse section through the graft reconstructed in Fig. 11C; see Fig. 11C for section orientation. Arrows indicate the mediolateral extent of the quail graft in the lateral wall of the midbrain. ×200.

Fig. 14. Transverse sections through either the graft reconstructed in Fig. 11D (Fig. 14A) or a similar graft (Fig. 14B); see Fig. 11D for section orientation. Arrows indicate the mediolateral extent of the quail graft in the lateral wall of the hindbrain; arrowhead indicates quail cells in the lateral wall of the spinal cord. ×200.

Are forces for neural plate shaping generated intrinsically or extrinsically?

Two lines of evidence suggest that neural plate shaping is the result of forces generated largely (if not exclusively) within the neural plate. The first comes from studies in which the neural plate was partially isolated *in vitro* from surrounding structures prior to shaping (Schoenwolf, 1988; Schoenwolf *et al.* 1989*b*). Normal shaping, but not bending, still occurs in isolation from lateral tissues (i.e. surface ectoderm; somitic, nephrotomic and lateral plate mesoderm; and lateral endoderm). Similarly, caudal tissues (i.e. primitive streak, including Hensen's node; postnodal neural plate tracts; preinvoluted and involving mesoblast; and caudal endoderm) are not required for shaping.

The second line of evidence comes from studies in which the cytoskeleton was disrupted with known inhibitors. Observations and morphometric analyses of the amphibian (Burnside & Jacobson, 1968) and chick (Schoenwolf, 1985) neural plates revealed that neural plate *thickening* (a process of neuroepithelial cell elongation not stratification) is correlated spatially and temporally with neural plate *narrowing*. Modeling studies suggested that these two events of neural plate shaping are linked causally (Jacobson & Gordon, 1976; Schoenwolf, 1985). This hypothesis was tested by depolymerizing neural plate paraxial microtubules and assessing its effect on neural plate thickening and narrowing (Schoenwolf & Powers, 1987). The results supported the conclusions of previous studies (reviewed by Karfunkel, 1974) that cell elongation is mediated in large part (but not exclusively) by paraxial microtubules and provided direct evidence that cell elongation acts in neural plate narrowing. However, the neural plate narrows by 50 % during its shaping, and cell elongation alone would be expected to generate only about a 15 % reduction in width (calculated from the data of Schoenwolf, 1985; the approximate 30 % increase in cell height that occurs during shaping would result in an approximate 15 % decrease in cell diameter if cell volume, calculated as if the cell were a cylinder, remained constant). Therefore, because 35 % of the reduction in neural plate width is unaccounted for other factors must be involved. The results of the present study show that cell rearrangement is a major player in this process (see below).

What is the role of cell rearrangement in neural plate extension?

In the present study, we provide evidence that cell rearrangement occurs during neural plate shaping. By rearrangement we are referring to what others have called intercalation (see Keller & Hardin, 1987: Fig. 1). Such rearrangement would result in the interdigitation of adjacent tiers of cells, so that the lateral edges of the neural plate would merge toward the midline. One round of rearrangement would result in the halving of the width of the plate and the doubling of its length.

What is the evidence that cell rearrangement occurs? The observations that grafts at site 'a' remain on the midline, those at site 'b' move toward the midline, and those at both sites 'a' and 'b' taper craniocaudally provide circumstantial evidence. Further circumstantial evidence is provided by the demonstration that marked cells in the lateral regions of the neural plate, obtained by injection of the avian epiblast with a cell tracer, are displaced toward the midline and those within the midline are displaced caudally (Schoenwolf & Sheard, 1989). Direct evidence is provided by the present study in which it was shown that the number of quail cells per transverse sectional level decreases within the midcraniocaudal extent of the graft and that gaps occur within the grafts at their caudal ends. Such a decrease in cell number is unlikely an artifact produced by misalignment of graft axes with respect to those of the host, because grafts contributing to the same levels of the neuraxis consistently showed similar behavior despite the fact that in some cases axes would be expected to be aligned but not in others.

How much cell rearrangement occurs? Counts of the numbers of cells in transverse sections through the midcraniocaudal extents of the grafts compared to the numbers of cells in the diameters of the plugs revealed that 2 rounds of cell rearrangement occur during neurulation (Table 4). However, this value is an average: no net mediolateral cell rearrangement occurs at cranial levels of the neural plate, where the latter expands laterally during its shaping (Schoenwolf, 1985; Schoenwolf & Powers, 1987), and near the caudal end of the neural plate, where few cells occupy the width of the graft, significantly more than 2 cell rearrangements likely occur.

What is the role of cell division in neural plate extension?

For amphibian embryos, in which little cell division and no cell growth occur during neurulation (Gillette, 1944), it is likely that cell rearrangement is the major factor underlying neural plate extension (Schroeder, 1971; Jacobson & Gordon, 1976). However, in higher vertebrates, substantial cell division occurs within the neural plate during neurulation (Langman *et al.* 1966; Tuckett & Morriss-Kay, 1985; Smith & Schoenwolf, 1987, 1988). Thus, it would be expected that neural plate extension in birds and mammals involves cell division in addition to cell rearrangement.

In the studies most germane to the present investigation, the flat neural plate of the chick (i.e. at stage 4) was shown to have a cell cycle length of about 8 h (Smith & Schoenwolf, 1987, 1988). Cell cycle length (including both its S and non-S portions, but not its M phase) increases for prospective M cells (to about 12 h) as the notochord forms and establishes apposition with their bases, but it remains unaltered for L cells. Thus, over a 24 h period, neural plate cells would be expected to undergo between 2–3 rounds of cell division. However, it is possible that this expectation yields a value that is too high, because cell cycle length generally increases with advance in developmental age. Therefore, a single population of cells (e.g. L cells of the midbrain) probably has a longer cycle at the closed neural tube stage (stages 10–11) than at flat or bending neural plate stages.

Our present results, based on determining the numbers of cells in grafts at 8, 12, 18 and 24 h postgrafting and comparing these numbers to the numbers of cells present in plugs, suggest that 2 rounds of cell division occur on the average over the 24 h period between late stage 3 and stages 10–11. However, it is possible that our counts of graft cell number were slightly underestimated for four reasons: (1) some cells could be lost from the graft due to cell death induced by the trauma of the grafting procedure; (2) some cells could be lost from the neuroepithelium by their migration to the mesenchyme from the cut edges of the graft prior to healing; (3) extensive cell rearrangement near the caudal end of the graft could lead to underestimation of cell numbers because single quail cells in a predominantly chick field can be more difficult to detect; and (4) culturing, trauma from grafting, or healing could lengthen the cell cycle, thereby decreasing the number of progeny generated. Also, the number of rounds of cell division was rounded to the nearest whole number (i.e. 2), but for grafts at both sites 'a' and 'b,' a 3rd round of cell division was initiated during the 24 h postgrafting period (Table 3). Thus, by comparing our present results with those obtained previously (Smith & Schoenwolf, 1987, 1988), we must conclude that a minimum of 2 rounds of cell division and a maximum of 3 occur during neurulation.

Our present results, in conjunction with others obtained previously (Schoenwolf, 1985), also suggest that the *direction* of cell division differs among various craniocaudal levels of the neuraxis. Portions of grafts that contribute to the forebrain (and to the lateral midbrain) expand laterally, whereas those that contribute to more caudal levels of the neuraxis exhibit marked mediolateral narrowing. The intact neural plate as a whole exhibits a similar expansion and narrowing, as revealed by reconstructions of the shapes of neural plates from serial sections at various stages (Schoenwolf, 1985: Fig. 8). Based on differences in the numbers of quail cells per transverse sectional level between cranial levels of the neural plate and the remainder of the neural plate, it seems likely that cell division is directed mainly within the transverse plane in the cranial portion of the neural plate and within the longitudinal plane at more caudal levels. This would explain why 2 rounds of cell division and 2 rounds of cell

rearrangement result in only 3 rounds of craniocaudal extension rather than 4 (Table 4) and why in grafts contributing principally to the forebrain, cell number doubles but graft length remains virtually constant.

Modeling of the factors involved in neural plate shaping

Our present and previous studies, as well as those of other investigators, have revealed three factors that act during neural plate shaping: (1) microtubule-mediated neuroepithelial cell elongation without loss of volume, thereby assisting in neural plate thickening and narrowing; (2) cell division, resulting in lateral expansion of the cranial levels of the neural plate and craniocaudal extension of the remainder of the neuraxis; and (3) mediolateral cell rearrangement, resulting in craniocaudal extension and mediolateral narrowing of the neural plate. How might these factors interact during neural plate shaping? Modeling studies can provide some insight into this question as well as identify the required assumptions that can be tested in future studies.

Fig. 15 shows a model that is consistent with the available data. Fig. 15A represents the neural plate at stages 3–4 as viewed from its apical side. Its width is greater than its length. Between stages illustrated by Fig. 15A and B, neuroepithelial cells elongate dorsoventrally, increasing their heights by a factor of about 30 % (1·3-fold, Schoenwolf, 1985). Because cell volume is assumed to remain constant, it would be expected, if cells are shaped like cylinders, that cell diameter would decrease by about 15 % (1·14 fold, Schoenwolf, 1985). This reduction in diameter would reduce the length of the neural plate as well as its width, but such a reduction in length has not been observed, suggesting that it is compensated for by concomitant cell rearrangement, cell division, change in cell shape, or other uncharacterized events. Between stages illustrated by Fig. 15B and C, 1 round of cell division occurs within the transverse plane. Between stages illustrated by Fig. 15C and D, 1 round of cell rearrangement occurs within the more caudal part of the neural plate (i.e. in the non-forebrain levels). Between stages illustrated by Fig. 15D and E, a second round of cell division occurs, with some cells dividing within the transverse plane and some within the longitudinal plane. Cell division in the transverse plane would account for the normally occurring lateral expansion of the forebrain and midbrain levels (Schoenwolf, 1985: Fig. 8). Between stages illustrated by Fig. 15E and F, approximately 1/2 round of cell rearrangement occurs, again in the more caudal part of the neural plate (i.e. caudal to the midbrain). This is repeated between stages illustrated by Fig. 15F and G.

Fig. 15H represents a neural plate with a size and shape mimicking those at stages 10–11 (Schoenwolf, 1985). To create this model, we have added 1/4 round of cell division (i.e. 8 of 32 cells divide to result in a total of 40 cells), principally within the longitudinal plane. This was done because our results suggest that more than 2 and less than 3 rounds of cell divisions occur. The model illustrated by Fig. 15H has the correct volume (5-fold that at stages 3–4) and thickness (1·3-fold that at stages 3–4). It also closely approximates the correct average width, because in control embryos, the width decreases 50 % between stages 4 and 11 (Schoenwolf, 1985) and in the model the width decreases 47 % (average cell number in the width of the model is reduced from 4 to 2·5 and cell diameter is reduced by 15 % due to cell elongation). Finally, the model approximates the correct length of the neural plate (6·8-fold increase as compared to that at stages 3–4), but this value is underestimated (the length of the neural plate of control embryos actually increases 8·7-fold between stages 4–11). There are three explanations for this discrepancy, each of which also accounts for the slight underestimation of the width reduction by the model: (1) somewhat more cell rearrangement might occur than modeled; (2) changes might occur in cell or extracellular volume; and (3) cell profiles might become anisotropic, so that their apices transform from circular to oval (i.e. profiles might narrow mediolaterally and

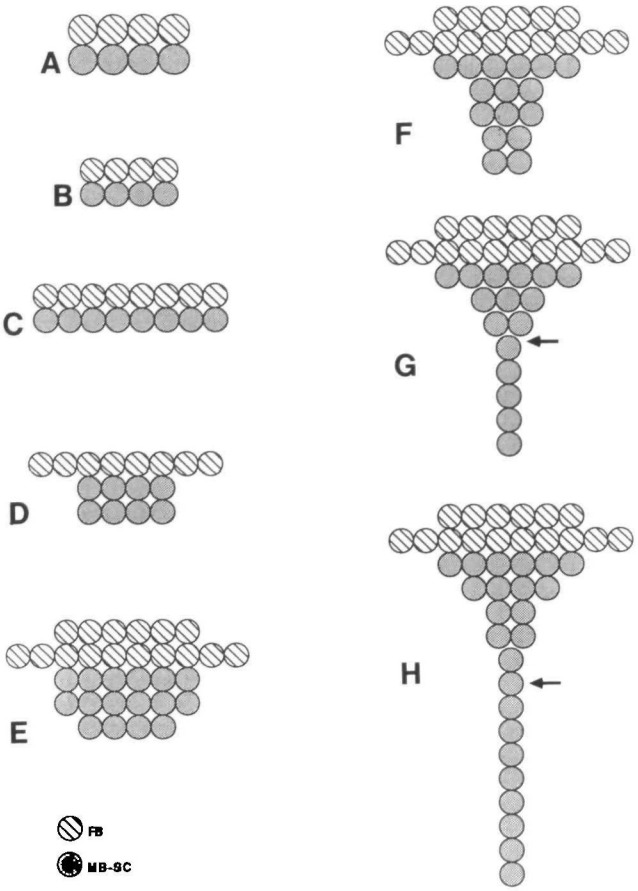

Fig. 15. Model showing one possible way in which an approximate 30 % increase in neuroepithelial cell height (and a corresponding approximate 15 % decrease in cell diameter so that cell volume remains constant), 2–3 rounds of cell division and 2 rounds of cell rearrangement could result in a neuraxis with approximately the correct size and shape. Arrows indicate the levels assessed to determine the amount of cell rearrangement (i.e. the arrows mark the midcraniocaudal extents of the grafts). See Discussion for an explanation of the various steps.

lengthen craniocaudally without changing cell volume, as modeled by Schoenwolf & Powers, 1987: Fig. 14D).

In conclusion, the model presented in Fig. 15 shows one possible way in which an approximate 30% increase in neuroepithelial cell height, 2–3 rounds of cell division, and 2 rounds of rearrangement might join forces to effectuate neural plate shaping. Its value is not in its exact details. Rather, it provides evidence in support of the hypothesis that these three processes play obligatory roles in neural plate shaping, and it aids in our conceptualization of how this complex developmental event might occur.

We gratefully acknowledge the superb technical assistance of Maggie Kasten and Jodi Smith and the dedicated secretarial assistance of Lisa Burkholder. This research was supported by grant no. NS18112 from the NIH. ISA's stay at the University of Utah was supported by a grant from the Junta de Extremadura and the Universidad de Extremadura, Spain.

References

ABERCROMBIE, M. (1946). Estimation of nuclear population from microtome sections. *Anat. Rec.* **94**, 239–247.

BURNSIDE, B. (1973). Microtubules and microfilaments in amphibian neurulation. *Am. Zool.* **13**, 989–1006.

BURNSIDE, B. & JACOBSON, A. G. (1968). Analysis of morphogenetic movements in the neural plate of the newt *Taricha torosa*. *Devl Biol.* **18**, 537–552.

GILLETTE, R. (1944). Cell number and cell size in the ectoderm during neurulation (*Amblystoma maculatum*). *J. exp. Zool.* **96**, 201–222.

GORDON, R. (1985). A review of the theories of vertebrate neurulation and their relationship to the mechanics of neural tube birth defects. *J. Embryol. exp. Morph.* **89 Supplement, 229–255.**

HAMBURGER, V. & HAMILTON, H. L. (1951). A series of normal stages in the development of the chick embryo. *J. Morph.* **88**, 49–92.

JACOBSON, A. G. & GORDON, R. (1976). Changes in the shape of the developing vertebrate nervous system analyzed experimentally, mathematically and by computer simulation. *J. exp. Zool.* **197**, 191–246.

KARFUNKEL, P. (1974). The mechanisms of neural tube formation. *Int. Rev. Cytol.* **38**, 245–271.

KELLER, R. E., DANILCHIK, M., GIMLICH, R. & SHIH, J. (1985). The function and mechanism of convergent extension during gastrulation of *Xenopus laevis*. *J. Embryol. exp. Morph.* **89 Supplement**, 185–209.

KELLER, R. E. & HARDIN, J. (1987). Cell behavior during active cell rearrangement: Evidence and speculation. *J. Cell Sci. Suppl.* **8**, 369–393.

LANGMAN, J., GUERRANT, R. L. & FREEMAN, B. G. (1966). Behavior of neuro-epithelial cells during closure of the neural tube. *J. comp. Neurol.* **127**, 399–412.

LEDOUARIN, N. M. (1982). *The Neural Crest.* Cambridge University Press, London.

LILLIE, R. D. (1965). *Histopathologic Technic and Practical Histochemistry*, pp. 149–150, 270. McGraw-Hill: New York.

MARTINS-GREEN, M. (1988). Origin of the dorsal surface of the neural tube by progressive delamination of epidermal ectoderm and neuroepithelium: Implications for neurulation and neural tube defects. *Development* **103**, 687–706.

MORRISS-KAY, G. M. (1981). Growth and development of pattern in the cranial neural epithelium of rat embryos during neurulation. *J. Embryol. exp. Morph.* **65**, 225–241.

MORRISS-KAY, G. M. & TUCKETT, F. (1987). Fluidity of the neural epithelium during forebrain formation in rat embryos. *J. Cell Sci. Suppl.* **8**, 433–449.

NEW, D. A. T. (1955). A new technique for the cultivation of the chick embryo *in vitro*. *J. Embryol. exp. Morph.* **3**, 320–331.

SCHOENWOLF, G. C. (1982). On the morphogenesis of the early rudiments of the developing central nervous system. *Scanning Electron Microsc.* **1982 (I)**, 289–308.

SCHOENWOLF, G. C. (1985). Shaping and bending of the avian neuroepithelium: Morphometric analyses. *Devl Biol.* **109**, 127–139.

SCHOENWOLF, G. C. (1988). Microsurgical analyses of avian neurulation: Separation of medial and lateral tissues. *J. comp. Neurol.* **276**, 498–507.

SCHOENWOLF, G. C., BORTIER, H. & VAKAET, L. (1989*a*). Fate mapping the avian neural plate with quail/chick chimeras: Origin of prospective median wedge cells. *J. exp. Zool.* **249**, 271–278.

SCHOENWOLF, G. C., EVERAERT, S., BORTIER, H. & VAKAET, L. (1989*b*). Neural plate- and neural tube-forming potential of isolated epiblast areas in avian embryos. *Anat. Embryol.* (in press).

SCHOENWOLF, G. C., FOLSOM, D. & MOE, A. (1988). A reexamination of the role of microfilaments in neurulation in the chick embryo. *Anat. Rec.* **220**, 87–102.

SCHOENWOLF, G. C. & POWERS, M. L. (1987). Shaping of the chick neuroepithelium during primary and secondary neurulation: Role of cell elongation. *Anat. Rec.* **218**, 182–195.

SCHOENWOLF, G. C. & SHEARD, P. (1989). Shaping and bending of the avian neural plate as analysed with a fluorescent-histochemical marker. *Development* **105**, 17–25.

SCHROEDER, T. E. (1970). Neurulation in *Xenopus laevis*. An analysis and model based upon light and electron microscopy. *J. Embryol. exp. Morph.* **23**, 427–462.

SCHROEDER, T. E. (1971). Mechanisms of morphogenesis: The embryonic neural tube. *Int. J. Neurosci.* **2**, 183–198.

SMITH, J. L. & SCHOENWOLF, G. C. (1987). Cell cycle and neuroepithelial cell shape during bending of the chick neural plate. *Anat. Rec.* **218**, 196–206.

SMITH, J. L. & SCHOENWOLF, G. C. (1988). Role of cell-cycle in regulating neuroepithelial cell shape during bending of the chick neural plate. *Cell Tiss. Res.* **252**, 491–500.

SUZUKI, A. S. & HARADA, K. (1988). Prospective neural areas and their morphogenetic movements during neural plate formation in the *Xenopus* embryo. II. Disposition of transplanted ectoderm pieces of *X. borealis* animal cap in prospective neural areas of albino *X. laevis* gastrulae. *Develop. Growth & Differ.* **30**, 391–400.

TUCKETT, F. & MORRISS-KAY, G. M. (1985). The kinetic behaviour of the cranial neural epithelium during neurulation in the rat. *J. Embryol. exp. Morph.* **85**, 111–119.

(Accepted 12 April 1989)